Rotational and vibrational effects in the $E\,^1\Sigma_g^+$–$X\,^1\Sigma_g^+$ two-photon transitions of H_2, HD, and D_2

Winifred M. Huo
NASA Ames Research Center, Moffett Field, California 94035
Klaus-Dieter Rinnen[a] and Richard N. Zare
Department of Chemistry, Stanford University, Stanford, California 94305

(Received 25 January 1991; accepted 26 March 1991)

A theoretical study is reported for the dependence of the $E, F\,^1\Sigma_g^+$–$X\,^1\Sigma_g^+$ ($v_E = 0$, v_X) Q-branch two-photon transitions on the initial vibrational and rotational quantum numbers v_X and J for H_2, HD, and D_2. The magnitude of the two-photon transition moment $|M_{fo}|$ increases with v_X between 0 and 2, then decreases rapidly at higher v_X. This behavior is ascribed to (constructive and destructive) interference effects in the two-photon transition, which vary with the nodal behavior of the initial-state vibrational wave function. The J dependence of $|M_{fo}|$ is most strongly affected by the changes in vibrational wave functions caused by centrifugal distortion of the vibrational potentials. At low to intermediate J, the Franck–Condon overlap improves, resulting in a slow, monotonic increase of $|M_{fo}|$ with J. At higher J, resonant tunneling between the inner and outer wells of the E, F state introduces sharp variations in the $|M_{fo}|$ structure. Near the top of the barrier, nonresonant tunneling in the E-state vibrational wave function causes a general decrease in $|M_{fo}|$ with J.

I. INTRODUCTION

Resonance-enhanced multiphoton ionization (REMPI) has been used to study product distributions in state-specific chemical reactions[1–6] and internal state distributions in high-temperature plasmas.[7] To make REMPI detection quantitative, the ion signal must be related to (v'', J'') population. Since several simple chemical reactions of current interest involve H_2 or its isotopes, we have undertaken a combined theoretical and experimental study of the rovibrational branching ratios in the 2 + 1 REMPI of H_2, HD, and D_2 with the intermediate resonant step a Q-branch two-photon transition to the lowest vibrational level of the inner well of the $E, F\,^1\Sigma_g^+$ state, i.e., $v_E = 0$. In this paper, we consider the v'', J'' dependence of the $E\,^1\Sigma_g^+$–$X\,^1\Sigma_g^+$ two-photon transition, the first step in the REMPI process. An accompanying experimental paper (Paper II)[8] describes the experimental determinations of the v'', J'' branching ratios from ion signals and discusses the conditions under which these branching ratios can be compared with the theoretical ratios deduced from the first step in the REMPI process. Results of our study on HD have been reported previously for a more limited range of J''.[9]

Generally, the dependence of the REMPI cross section on J'' is small and varies smoothly. However, the double-minima nature of the E, F state[10,11] introduces large and sudden variations in the J'' dependence of the cross sections. Kolos and Wolniewicz[11] were the first to note that the ordering of the vibrational levels in the inner and outer wells is J dependent. The lowest vibrational level of the E, F state shifts from the inner well, $v_E = 0$, to the outer well, $v_F = 0$, for $J > 3$. Senn and Dressler[12] studied the resonant tunneling between the inner and outer wells and its effect on the rovibrational structures in the E, F state. Marinero, Vasudev, and Zare[13] observed non-Franck–Condon intensity distributions in the two-photon transitions from $X\,^1\Sigma_g^+$, $v'' = 0$ to the vibrational levels of the inner and outer wells of the E, F state. This non-Franck–Condon distribution was also found in the *ab initio* calculations of Huo and Jaffe.[14] Our previous investigation on HD[9] for $J'' \leqslant 14$ did not show any effect of tunneling. In the present study, we follow the Q-branch two-photon transition, E–X ($v_E = 0$, v_X). This study is carried out from $J = 0$ to the highest J value for which the $v_E = 0$ level is either at or just above the top of the barrier. Since our calculations are performed at higher J values, we observe not only resonant tunneling when the vibrational levels from the inner and outer wells are nearly degenerate but also nonresonant tunneling effects when the vibrational level is near the top of the barrier. We find that the tunneling effect causes a sudden, large change in the two-photon absorption cross section that results in pronounced irregularities in the two-photon transition moment as a function of rotation.

II. THE Q-BRANCH TWO-PHOTON TRANSITION MOMENT AND ITS J DEPENDENCE

The two-photon absorption rate (in s^{-1}) is given by

$$w_{fo} = (2\pi)^3(\hbar c)^{-2}N_0|M_{fo}|^2I^2g(\omega_{fo} - 2\omega)G^{(2)} \qquad (1)$$

for the case of a single photon frequency ω. Here I is the single-color field intensity (in energy per area per second), N_0 is the Boltzmann population of the molecule in the initial state, $g(\omega_{fo} - 2\omega)$ is the normalized line shape function, and $G^{(2)}$ is a photon statistical factor. The two-photon transition moment M_{fo} can be expressed[15] as

$$M_{fo} = \sum_i \frac{\langle f|\mathbf{r}\cdot\hat{\epsilon}|i\rangle\langle i|\mathbf{r}\cdot\hat{\epsilon}|0\rangle}{(E_i - E_0 - \hbar\omega)}, \qquad (2)$$

where the summation is over all rovibronic states that can be coupled to the initial and final states by electric-dipole-allowed transitions. For a diatomic molecule in Hund's case

[a] Present address: AT&T Bell Laboratories, Room 1D354, 600 Mountain Avenue, Murray Hill, New Jersey 07974.

(a) excited by linearly polarized light, the rotational line strength in the Q branch of a Σ–Σ transition can be expressed[16] as

$$M_{fo} = \left(\frac{1}{9}\,|M^{I}_{fo}|^2 + \frac{4J(J+1)}{45(2J-1)(2J+3)}\,|M^{A}_{fo}|^2\right)^{1/2}. \qquad (3)$$

Here $J = J' = J''$. The isotropic and anisotropic two-photon moments are

$$M^{I}_{fo} = M^{\parallel}_{fo} + 2M^{\perp}_{fo} \qquad (4a)$$

and

$$M^{A}_{fo} = M^{\parallel}_{fo} - M^{\perp}_{fo}. \qquad (4b)$$

The parallel component of the two-photon transition moment is given by

$$M^{\parallel}_{fo} = \sum_i \sum_{v_i} \frac{\langle \phi_f(\mathbf{r},R)\chi_{v'J}(R)|z|\phi_i(\mathbf{r},R)\chi_{v_iJ_i}(R)\rangle\langle \phi_i(\mathbf{r},R)\chi_{v_iJ_i}(R)|z|\phi_0(\mathbf{r},R)\chi_{v''J}(R)\rangle}{E_{iv_iJ_i} - E_{0v''J} - \hbar\omega}, \qquad (5)$$

where $\mathbf{r}$ represents the totality of electronic coordinates and R the internuclear separation. The definition for $M^{\perp}_{fo}$ is analogous to Eq. (5), with the operator z replaced by $1/\sqrt{2}(x \pm iy)$.

The present calculations of the two-photon transition moments follow a previously described procedure.[9,14] A total of 124 intermediate electronic states are used in the summation. Explicit summation is carried out over the vibrational levels of the lowest four electronic states, $B\,^1\Sigma_u^+$, $C\,^1\Pi_u$, $B'\,^1\Sigma_u^+$, and $D\,^1\Pi_u$; for the remainder, a nuclear sudden approximation[9] is used. Figure 1 depicts the potential curves of these four states and the X and E, F states. In the summation over vibrational levels, we include all bound and continuum contributions until convergence is obtained. Vibrational wave functions were obtained from numerical solutions of the one-dimensional Schrödinger equation. The present treatment differs from previous studies[9,14] in that it uses adiabatic rather than Born–Oppenheimer potentials. The effect of the adiabatic correction on the two-photon transition moment is small except when resonant tunneling becomes important in the E, F state. Under those circumstances, a small change in the relative spacing of the neighboring v_E and v_F levels has a pronounced effect on the extent of tunneling, which in turn changes the magnitude of the two-photon transition moment. The adiabatic potential for the X state is taken from the compilation of Schwartz and Le Roy[17] and the adiabatic potentials for the (E, F), B, C, B', and D states from the work of Wolniewicz and Dressler.[18,19]

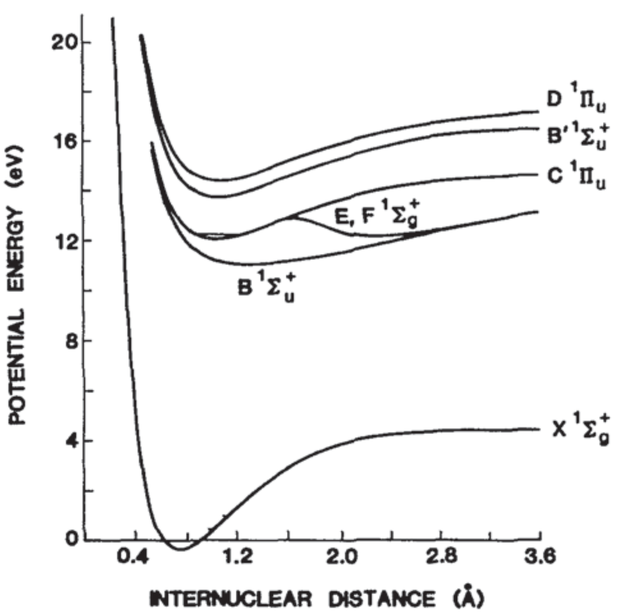

FIG. 1. Potential energy curves for the $X\,^1\Sigma_g^+$, $E,F\,^1\Sigma_g^+$, $B\,^1\Sigma_u^+$, $C\,^1\Pi_u$, $B'\,^1\Sigma_u^+$, and $D\,^1\Pi_u$ states of H_2. The $v_x = 0,1,2$ and $v_E = 0$ vibrational levels are indicated.

As seen from Eqs. (3) and (5), M_{fo} depends on J in three ways: (1) explicit dependence through the two-photon rotational line strength factor; (2) dependence on the energy difference $E_{iv_iJ_i} - E_{ov''J}$; and (3) implicit dependence through the centrifugal potential used in determining the vibrational wave functions $\chi_{vJ}(R)$. Because the centrifugal potential, $\hbar J(J+1)/2\mu R^2$, decreases with increasing R, centrifugal distortion raises the minimum of the potential curve with respect to its asymptote and changes the relative well depths in a double-minima potential. For this reason, centrifugal distortion has a much stronger effect on the E, F state than on others. The $v_E = 0$ level of H_2 as a function of J changes from being the lowest vibrational level of the E, F state at $J = 0$ to the ninth vibrational level at $J = 21$, where it is above the barrier. Thus the $v_E = 0$ level crosses a v_F level nine times between $J = 0$ and $J = 21$. Near the crossing point, the theoretical M_{fo} and the experimental ion intensity show strong variations in their J dependence as a result of the perturbation of the $v_E = 0$ level by the nearest v_F level, i.e., resonant tunneling occurs. Also, as J approaches 21, the $v_E = 0$ level approaches the top of the barrier. Since its wave function is no longer localized in the inner well, nonresonant tunneling occurs.

Senn and Dressler[12] studied the effect of resonant tunneling on the term values of the v_E and v_F levels using a semiclassical treatment. They calculated the fractional value of J at which a pair of nearby v_E and v_F levels becomes resonant and thus determined the interaction energy of the pair. Because we are interested in transition probabilities instead of term values, we sought to obtain a qualitative estimate in the change of transition probabilities under resonant tunneling using a quantum-mechanical two-state treatment. Consider a zero-order approximation of the double-well potential problem as two completely localized wave functions for the inner and outer wells ψ_1 and ψ_2 obtained with the barrier raised artificially high. Such localized wave functions are good approximations to ψ_E and ψ_F at low v and J levels. The perturbation potential V is the actual barrier in the E, F potential. Thus an improved approximation to ψ_E and ψ_F is

$$\psi_E = c_1\psi_1 + c_2\psi_2 \tag{6}$$

and

$$\psi_F = c_1'\psi_1 + c_2'\psi_2. \tag{7}$$

The energies of the two levels are obtained by solving the 2×2 matrix for its eigenvalues

$$E = \tfrac{1}{2}(E_1 + E_2) \pm \sqrt{\tfrac{1}{4}(E_1 - E_2)^2 + V_{12}^2}, \tag{8}$$

where E_1 and E_2 are related to the unperturbed energies ϵ_1 and ϵ_2 by

$$E_1 = \epsilon_1 + V_{11}, \tag{9}$$

$$c_2/c_1 = V_{12}/(E - E_2), \tag{10}$$

and

$$c_2'/c_1' = V_{12}/(E' - E_2). \tag{11}$$

Here E' is the second root in Eq. (8). This treatment is just the quantum-mechanical analog of the semiclassical treatment of Senn and Dressler. Since the wave functions ψ_1 and ψ_2 are defined to be localized and the potential V is outside the localized regions, V_{11}, V_{22}, and V_{12} are small. Unless the two levels are sufficiently close that $V_{12} \approx E_1 - E_2$, little mixing will occur between the two levels.

Equation (6) is an approximation of the exact ψ_E because the wave function inside the barrier is not adequately described by the superposition of two localized wave functions. Nevertheless, Eq. (9) can be used to estimate the effect of resonant tunneling on the two-photon transition moment. At low J values, the unfavorable Franck–Condon factor between the low-lying v_X and v_F levels means that the two-photon transition moment for F–X is much smaller than that for the E–X transition moment. This estimate has been borne out by experimental measurements[13] and theoretical calculations.[14] At $J=0$, the ratio between the two-photon transition moments for $v_E = 0 - v_X = 0$ and $v_F = 0$ $(v_{E,F} = 1) - v_X = 0$ is 1.0:0:0.001.[20] Since maximum mixing occurs when $c_2/c_1 = 1$, the E–X transition moment can at most decrease to 70% of its original value. As J increases, the v_F levels become more delocalized and the F–X transition moment becomes larger. Destructive interference between the two contributions may cause the resulting E–X transition moment to be less than 70% of its original value.

At high J, the $v_E = 0$ level is raised to near the top of the barrier, and nonresonant tunneling becomes important. Unlike the resonant case, this tunneling effect is independent of the location of the v_F levels. Even in the region where nonresonant tunneling is important, we still can find strong resonant tunneling effects when a v_F level is nearby. The combined effect of the two introduces further irregularities in the J dependence of the two-photon transition moment near J_{max}.

III. RESULTS AND DISCUSSION

We have determined the Q-branch two-photon transition moments for the $E,F\,{}^1\Sigma_g^+ - X\,{}^1\Sigma_g^+$ $(v_E = 0,\ v_X = 0–2)$ transitions for H_2 $(J = 0–21)$, HD $(J = 0–24)$, and D_2 $(J = 0–30)$. The results of these calculations are presented in Tables I–IV and Figs. 2–5. At $J=0$ the results for $v_X = 3$ to 6 are also included. In the following section we consider the v_X and J dependence of $|M_{fo}|^2$ separately.

TABLE I. $|M_{fo}|^2$ values for the H_2, HD, and D_2 Q-branch two-photon transitions $E,F\,{}^1\Sigma_g^+ - X\,{}^1\Sigma_g^+$ $(v_E = 0, J' = 0, v_X, J = 0)$.

v_X	$\vert M_{fo}\vert^2$ (a.u.)		
	H_2	HD	D_2
0	9.13	6.87	4.28
1	26.36	22.12	16.19
2	29.38	28.50	25.55
3	16.24	19.07	22.07
4	4.73	7.18	11.49
5	0.71	1.53	3.72
6	0.050	0.18	0.75

A. Two-photon transition moment as a function of v_X

The two-photon transition moments at $J=0$ are calculated as a function of v_X for $v_X = 0–6$ (Table I, Fig. 2). For all three isotopes, $|M_{fo}|^2$ increases sharply between $v_X = 0$ and $v_X = 2$ and then decreases rapidly at higher v_X. We have previously discussed the initial increase of $|M_{fo}|^2$ for HD as a constructive interference effect.[9] To understand the behavior of $|M_{fo}|^2$ in the range of v_X considered here, we present in Fig. 6 the one-photon transition moments for the B–X and E–B transitions of H_2, μ_{BX} and μ_{EB}, as a function of v_B. When either the initial or the final vibrational level is nodeless ($v_X = 0$ or $v_E = 0$), the oscillations in the one-photon transition moment function are simple. Note that the sign changes in the one-photon transition moment; this change reflects the nodal behavior of the B-state vibrational wave

TABLE II. $|M_{fo}|^2$ values for the Q-branch two-photon transitions H_2 $E,F\,{}^1\Sigma_g^+ - X\,{}^1\Sigma_g^+$ $(v_E = 0, v_X)$.

J	$\vert M_{fo}\vert^2$ (a.u.)		
	$v_X = 0$	$v_X = 1$	$v_X = 2$
0	9.13	26.36	29.37
1	9.15	26.47	29.54
2	9.20	26.61	29.71
3	9.26	26.83	29.98
4	9.34	27.12	30.36
5	9.44	27.48	30.82
6	9.56	27.91	31.39
7	9.68	28.34	31.97
8	9.85	28.97	32.83
9	10.02	29.60	33.70
10	10.18	30.28	34.61
11	10.36	31.06	35.73
12	9.66	29.82	34.00
13	10.89	32.87	38.17
14	8.77	26.38	31.06
15	11.62	35.47	41.38
16	11.49	35.21	42.06
17	11.65	37.00	42.15
18	12.05	38.84	48.56
19	9.26	31.62	39.00
20	6.28	25.59	38.94
21	8.63	33.58	49.84

TABLE III. $|M_{fo}|^2$ values for the Q-branch two-photon transitions HD $E, F\,{}^1\Sigma_g^+ – X\,{}^1\Sigma_g^+\ (v_E = 0, v_X)$.

J	$|M_{fo}|^2$ (a.u.) $v_X = 0$	$v_X = 1$	$v_X = 2$
0	6.87	22.12	28.50
1	6.89	22.20	28.62
2	6.91	22.28	28.74
3	6.95	22.41	28.92
4	6.99	22.59	29.19
5	7.04	22.81	29.53
6	7.11	23.07	29.92
7	7.19	23.37	30.39
8	7.27	23.72	30.92
9	7.36	24.10	31.53
10	7.45	24.51	32.20
11	7.56	24.97	32.93
12	7.66	25.46	33.76
13	7.84	26.04	34.53
14	7.88	26.53	35.63
15	7.93	27.10	36.41
16	8.32	28.07	37.74
17	3.92	14.93	19.61
18	8.85	30.18	41.00
19	8.65	30.65	41.49
20	7.54	27.60	38.38
21	9.08	33.11	47.47
22	8.72	31.24	45.91
23	5.10	18.91	33.76
24	6.51	27.16	46.20

TABLE IV. $|M_{fo}|^2$ values for the Q-branch two-photon transitions D_2 $E, F\,{}^1\Sigma_g^+ – X\,{}^1\Sigma_g^+\ (v_E = 0, v_X)$.

J	$|M_{fo}|^2$ (a.u.) $v_X = 0$	$v_X = 1$	$v_X = 2$
0	4.28	16.19	25.55
1	4.29	16.23	25.63
2	4.30	16.26	25.70
3	4.31	16.32	25.81
4	4.33	16.41	25.96
5	4.35	16.51	26.15
6	4.38	16.63	26.37
7	4.41	16.77	26.64
8	4.44	16.92	26.93
9	4.47	17.10	27.27
10	4.51	17.29	27.65
11	4.55	17.50	28.06
12	4.59	17.72	28.51
13	4.64	17.96	28.99
14	4.68	18.21	29.52
15	4.72	18.45	30.05
16	4.80	18.79	30.63
17	4.79	18.99	31.32
18	4.86	19.32	31.95
19	4.99	19.72	32.65
20	5.02	20.07	33.39
21	5.18	20.63	34.15
22	5.21	21.04	35.25
23	5.21	21.33	36.01
24	4.97	20.84	36.12
25	5.38	22.47	38.78
26	5.82	25.96	43.56
27	3.28	14.04	27.09
28	5.27	24.56	47.57
29	5.46	23.57	49.14
30	4.71	19.56	39.98

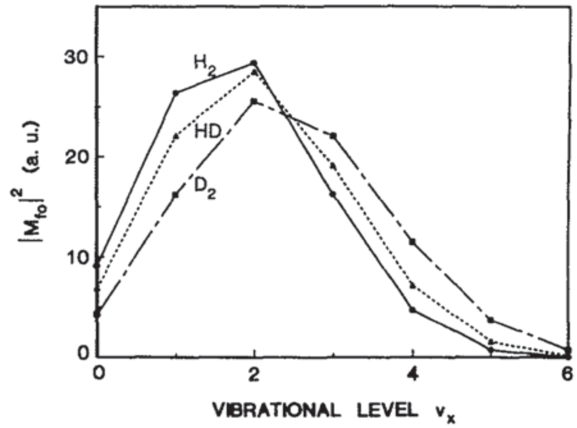

FIG. 2. The square of the E–$X\,(0,v_X)$ two-photon Q-branch transition moment $|M_{fo}|^2$ as a function of v_X at $J = 0$, for H_2, HD, and D_2.

function. As v_X increases, the ground state vibrational level also exhibits nodes and, consequently, damping occurs in the B–X transition moment function. The maximum transition moment (in magnitude) is at $v_B = 6$ for $v_X = 0$; the position of the maximum shifts to $v_B = 2$ for $v_X = 1$ and $v_B = 1$ for $v_X = 2$. For $v_X \geqslant 2$, the maximum of the transition moment is always at $v_B = 0$. For the E–B transition at $v_E = 0$, the largest transition moment occurs at $v_B = 0$. Its magnitude then decreases rapidly with v_B and becomes negligible above $v_B = 10$. Since a two-photon transition is a concerted process that involves the product of two one-photon transitions, we need to consider the overlap between the B–X and E–B transition moment functions. We note from Fig. 6 that the overlap of the two transition moments initially improves with increasing v_X and the magnitude of $M_{fo}^{\parallel}$ via the B state increases with v_X at low v_X. At higher vibrational excitations, however, the E–B and B–X transition moments move out of phase. This destructive interference diminishes the magnitude of $M_{fo}^{\parallel}$ via the B state. The $M_{fo}^{\parallel}$ curves in Fig. 7 reflect the constructive and destructive interference effects of the one-photon transition moments. At $v_X = 0$, the contributions to $M_{fo}^{\parallel}$ as a function of v_B are all negative; the maximum contribution (in magnitude) comes from the

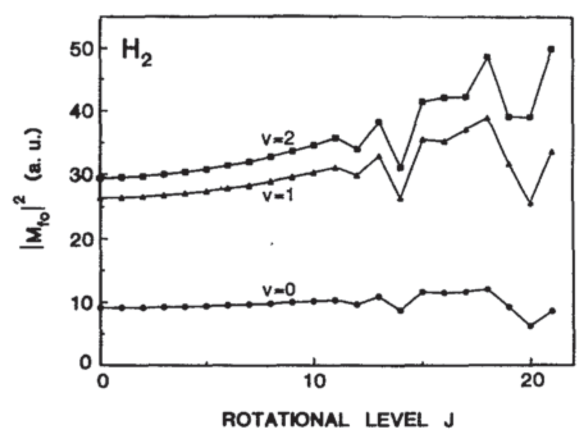

FIG. 3. The square of the H_2 E–$X\,(0,v_X)$ two-photon Q-branch transition moment, $|M_{fo}|^2$, as a function of J for $v_X = 0,1$, and 2.

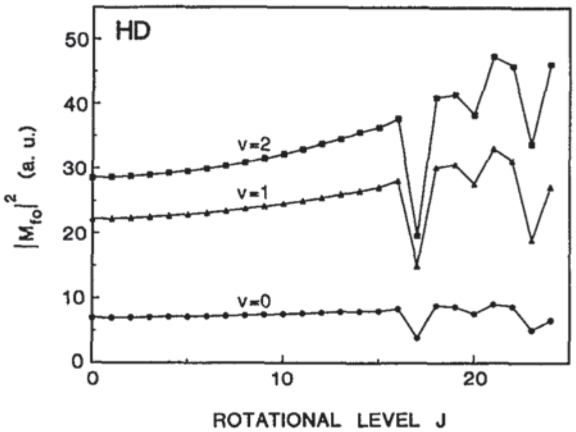

FIG. 4. The square of the HD E–X $(0,v_X)$ two-photon Q-branch transition moment, $|M_{fo}|^2$, as a function of J for $v_X = 0,1$, and 2.

$v_B = 2$ level. The position of the maximum shifts to $v_B = 1$ for $v_X = 1$ and 2. For $v_X \geqslant 2$, although the maximum (in magnitude) is still located at $v_B = 0$, positive contributions to $M_{fo}^{\parallel}$ develop, and the two-photon transition moment decreases in magnitude. Between $v_X = 3$ and 6, the magnitude of the positive extremum increases while its position shifts to lower v_B. At $v_X = 6$, a nearly complete cancellation of the negative and positive contributions occurs and $M_{fo}^{\parallel}$ is very small. Similar constructive and destructive interference effects are seen for other intermediate states; these effects account for the overall trend observed in $M_{fo}^{\parallel}$.

The preceding discussion has treated the E–X transition as a concerted two-photon process. An alternative argument, which is sometimes used to predict the trend of the v_X dependence of $|M_{fo}|^2$, assumes $|M_{fo}|^2$ to be proportional to the Franck–Condon (FC) factor of the E and X states. As a test of the FC argument, Table V compares the v_X dependence of $|M_{fo}|^2$ and the E–X FC factors for H_2. Table V shows that the FC argument indeed reproduces some of the qualitative features, such as the maximum at low v_X and the rapid decrease at higher v_X. However, the FC argument is quantitatively inaccurate because it places the position of the maximum at the wrong v_X and predicts a slower decrease than is observed at high v_X. These quantitative deficiencies result from treating the E–X excitation as a single step and neglecting the effect of the intermediate electronic states.

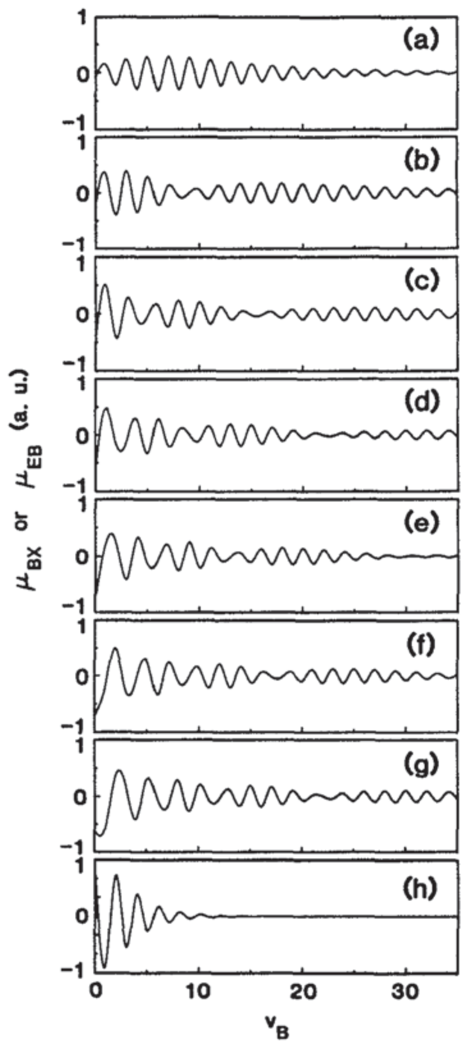

FIG. 6. The one-photon transition moments for H_2 as function of the vibrational quantum number v_B of the $B\,^1\Sigma_u^+$ state for the transitions (a) B–X $(v_B,0)$, (b) B–X $(v_B,1)$, (c) B–X $(v_B,2)$, (d) B–X $(v_B,3)$, (e) B–X $(v_B,4)$, (f) B–X $(v_B,5)$, (g) B–X $(v_B,6)$, and (h) E–B $(0,v_B)$.

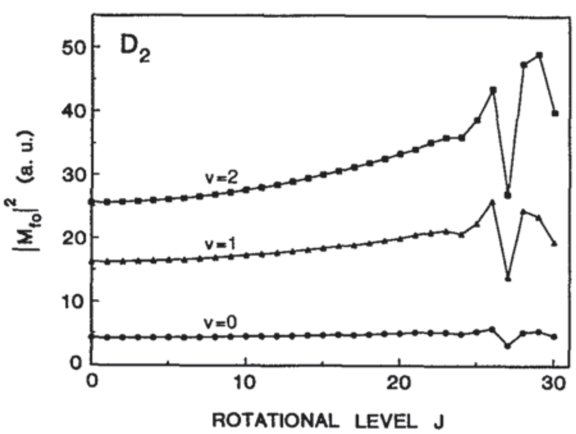

FIG. 5. The square of the D_2 E–X $(0,v_X)$ two-photon Q-branch transition moment, $|M_{fo}|^2$, as a function of J for $v_X = 0,1$, and 2.

B. Two-photon transition moment as a function of *J*

The two-photon transition moments for all three isotopes show a slow, monotonic increase as a function of J at low J (Figs. 3–5). The slopes of the $|M_{fo}|^2$ vs J curves are v_X dependent, with the $v_X = 2$ curve increasing fastest and the $v_X = 0$ curve virtually flat. At middle to high J, large, sudden dips in $|M_{fo}|^2$ are observed. For H_2 $v_X = 0$, 1, and 2, these dips occur at $J = 12$, 14, and 20. For HD, the minima occur at $J = 17$, 20, and 23, and for D_2 they are located at $J = 24$, 27, and 30. At higher J, in addition to these sharp minima, $|M_{fo}|^2$ generally decreases. The only exception is the $v_X = 2$ curve for H_2.

Section II discusses the three factors that determine the J dependence of $|M_{fo}|^2$: the rotational line strength factor, the energy-difference factor, and the centrifugal potential

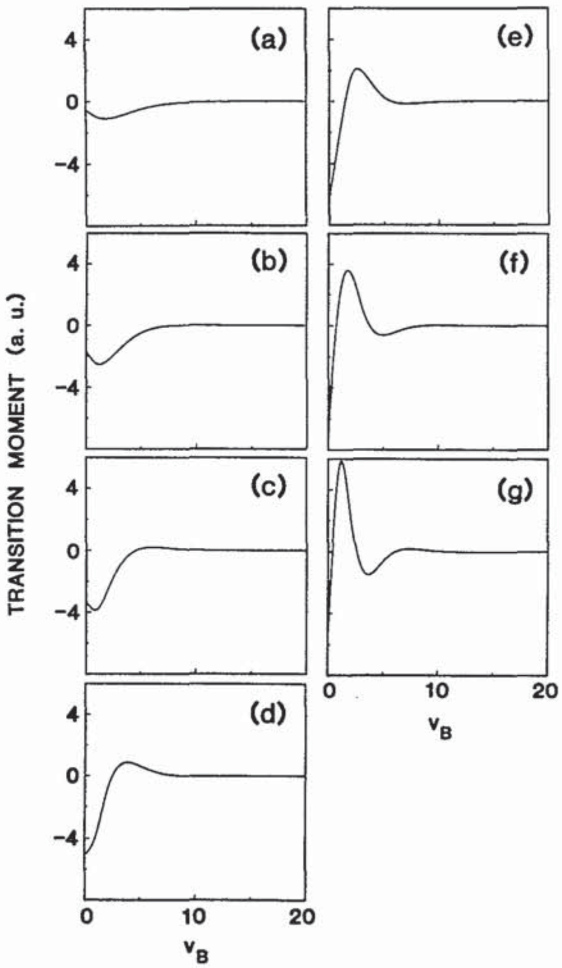

FIG. 7. The H_2 E,F–X $(0,v_X)$, $J=0$ two-photon Q-branch transition moment of H_2, $|M_{fo}|$, as a function of the vibrational quantum number v_B of the B state: (a) $v_X=0$, (b) $v_X=1$, (c) $v_X=2$, (d) $v_X=3$, (e) $v_X=4$, (f) $v_X=5$, and (g) $v_X=6$.

for the vibrational motion. The first factor, from the anisotropic term in M_{fo}, is largest as J increases from 0 to 1; for $J>1$ it slowly decreases with J, opposite to the observed trend at low and middle J. Examination of the relative magnitude of the isotropic and anisotropic contributions to M_{fo} reveals that $|M^I_{fo}|^2$ is at least ten times larger than $|M^A_{fo}|^2$. In addition, the coefficient multiplying $|M^I_{fo}|^2$ is at least three

TABLE V. Comparison of $|M_{fo}|^2$ values for the H_2 Q-branch transitions E, $F\,^1\Sigma_g^+$–$X\,^1\Sigma_g^+$ $(v_E=0,v_X,J'=0)$ with the corresponding E–X Franck–Condon factors.

v_X	$\|M_{fo}\|^2$ (a.u.)	FC factor
0	9.13	0.158
1	26.36	0.359
2	29.38	0.314
3	16.24	0.135
4	4.73	0.030
5	0.71	0.0034
6	0.050	0.0002

times larger than that for $|M^A_{fo}|^2$. Thus we conclude that the J dependence from the rotational line strength factor cannot account for the observed trends in $|M_{fo}|^2$.

Both the excitation frequency ω and the energy difference $E_{iv_iJ_i}-E_{ov''J}$ are J dependent. Since the ground state rotational constants for H_2 and its isotopes are larger than the corresponding values for the excited states, both ω and $E_{iv_iJ_i}-E_{ov''J}$ decrease with increasing J, a trend that results in a slow increase of M_{fo} with J [Eq. (2)]. This J dependence is partially responsible for the initially slow, monotonic increase in $|M_{fo}|^2$ but not the sharp minima or the decrease at high J.

The $J(J+1)$ dependence of the centrifugal potential directly affects the one-photon vibronic transition moments, which in turn affect M_{fo}. As discussed in Sec. II, the effect of centrifugal distortion should be smooth for all states except the E, F state, in which resonant and nonresonant tunneling can occur as J increases. In the region where tunneling is unimportant, centrifugal distortion shifts R_e to a slightly larger value. Although these shifts are small, their effect is the largest for the X state because it has the smallest R_e value. Thus the increase in the centrifugal potential improves the overlap between the X state and other states. As a result, M_{fo} increases slowly with J, as is observed in the region of low and intermediate J.

Section II ascribes the sharp variations in $|M_{fo}|^2$ to resonant tunneling in the E, F state. To determine the validity of this claim, we study the one-photon transition moments μ_{EC} (between $C\,^1\Pi_u$, $v_C=0$ and E, $v_E=0$) and μ_{FC} (between $C\,^1\Pi_u$, $v_C=0$ and the vibrational level of the F state closest to the $v_E=0$ level). Since the C-state potential curve nearly coalesces with the inner well of the E, F state (Fig. 1), the overlap between $v_C=0$ and $v_E=0$ is close to unity and the transition moment between these two levels is large. On the other hand, the transition moment between $v_C=0$ and the v_F level closest to $v_E=0$ is small. Any sudden changes in the magnitudes of these transition moments reflect a change in the coupling between the v_E and v_F levels. Figure 8(a) compares $|\mu_{EC}|$ and $|\mu_{FC}|$ for H_2. Every minimum in the $|\mu_{EC}|$ curve has a corresponding maximum in the $|\mu_{FC}|$ curve, which supports the conjecture that these minima and maxima are correlated as a result of resonant mixing between these two levels.

Note that the first two maxima in $|\mu_{FC}|$ do not appear to have corresponding minima in $|\mu_{EC}|$. They are also the two smallest maxima in the $|\mu_{FC}|$ curve, indicating a small mixing between v_E and v_F. For the first peak in $|\mu_{FC}|$, at $J=7$, a dip in $|\mu_{EC}|$ actually does exist but is too shallow to be discernible in the plot. For the second peak in $|\mu_{EC}|$, at $J=10$, the corresponding $|\mu_{EC}|$ does not have a minimum but shows instead a slight change in the slope of $|\mu_{EC}|$. Note that the magnitude of each dip is proportional to the magnitude of each peak, though less prominent.

Figure 9(a) compares the energy gap between the two levels ΔE and $|\mu_{FC}|$. Each dip in ΔE corresponds to a near crossing of a v_E and a v_F level. Also, each dip except the first in the ΔE curve has a corresponding peak in the $|\mu_{FC}|$ function. Equation (11) shows that the mixing of E-state charac-

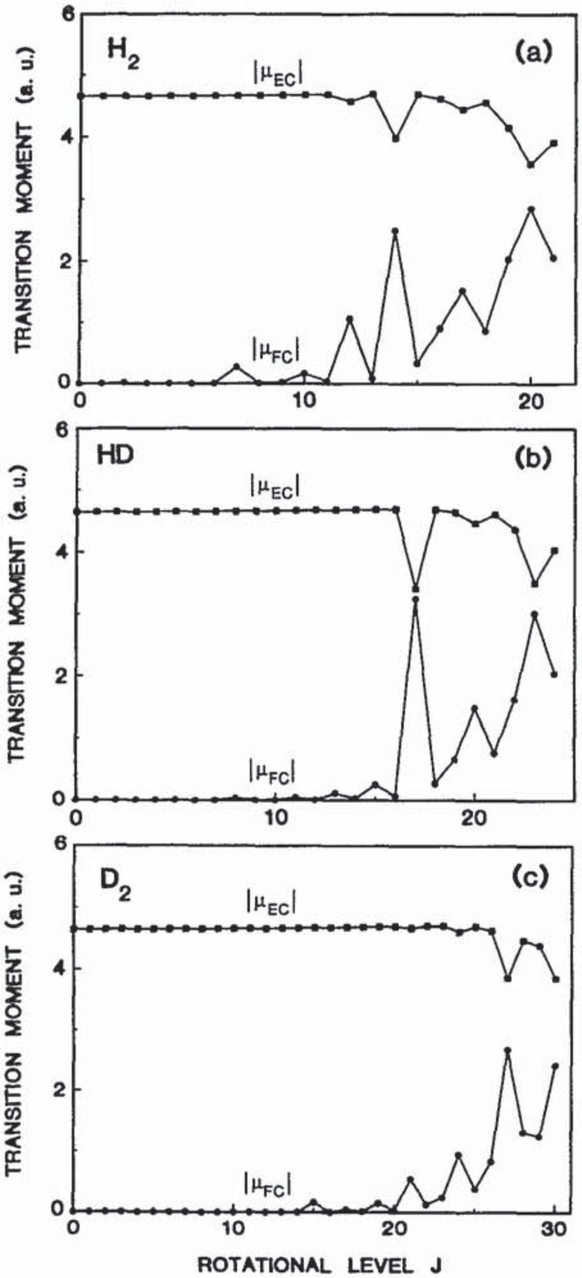

FIG. 8. Magnitudes of the E–C (0,0) and F–C (v_F,0) one-photon transition moments, $|\mu_{EC}|$ and $|\mu_{FC}|$, as a function of J for (a) H_2, (b) HD, and (c) D_2. The v_F level is the one closest to the $v_E = 0$ level at the value of J shown.

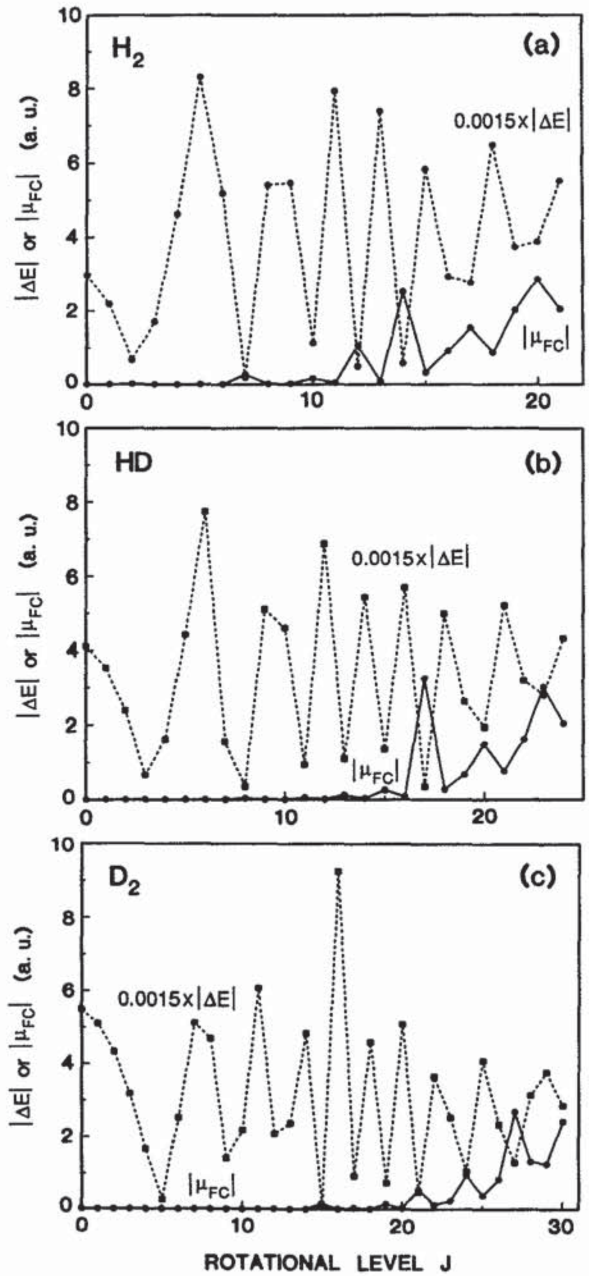

FIG. 9. The energy gap ΔE between $v_E = 0$ and the closest v_F level and the magnitude of the F–C (v_F,0) one-photon transition moment $|\mu_{FC}|$ as a function of J for (a) H_2, (b) HD, and (c) D_2.

ter in $|\mu_{FC}|$ depends on ΔE and V_{12}. The latter depends on both the width and the height of the barrier. Thus the closer the level is to the top of the barrier, the larger V_{12} becomes, as Fig. 9(a) clearly demonstrates. The first dip in ΔE has no corresponding peak in $|\mu_{FC}|$ because at $J = 2$ the v_F level under consideration is near the bottom of the well and V_{12} is too small to introduce any significant mixing with the v_E level. At $J = 7$, where the energy gap is smaller and V_{12} larger, $|\mu_{FC}|$ shows its first peak. As J increases, the v_F level approaches the top of the barrier, V_{12} grows in magnitude, and $|\mu_{FC}|$ generally increases. The highest peak in $|\mu_{FC}|$, at $J = 14$, is a combined result of a small ΔE and a large V_{12}.

Figure 10(a) compares $|M_{fo}|^2$ with $|\mu_{EC}|^2$ as a function of J for H_2. Both the positions and the magnitudes of the dips correspond well, except at $J = 17$. At that J value, $|\mu_{EC}|^2$ shows a definite dip, whereas $|M_{fo}|^2$ shows a shallow minimum at $J = 16$ instead of $J = 17$. This discrepancy is caused by the contribution from the $B'\,{}^1\Sigma_u^+$ intermediate state, which decreases faster than the contributions from other intermediate states, partly because the number of bound vibrational levels of that state decreases from 2 to 1. Since the contribution from $B'\,{}^1\Sigma_u^+$ is opposite in sign from the others, $|M_{fo}|^2$ is larger at $J = 17$ than at $J = 16$.

Figures 8(b), 9(b), and 10(b) compare $|\mu_{EC}|$ with $|\mu_{FC}|$, $|\mu_{FC}|$ with ΔE, and $|M_{fo}|^2$ with $|\mu_{EC}|^2$ for HD; the corresponding quantities for D_2 are presented in Figs. 8(c), 9(c), and 10(c). The general features of these comparisons are similar to those for H_2. Again, the variations in the one-

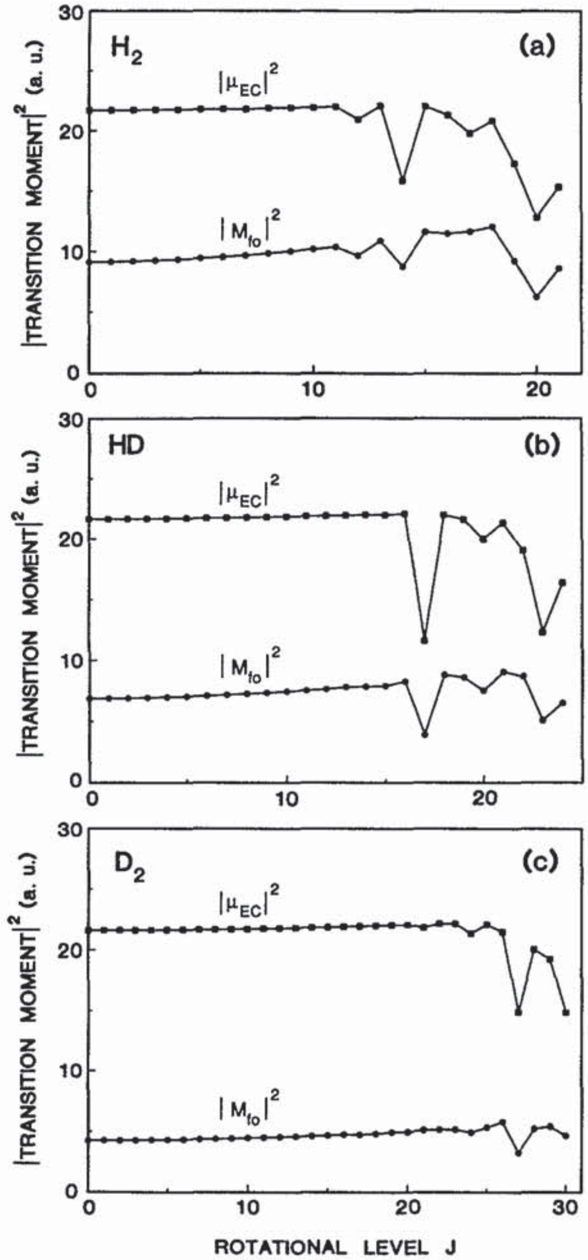

FIG. 10. Squares of the E–X (0,0) two-photon Q-branch transition moment $|M_{fo}|^2$ and E–C (0,0) one-photon transition moment $|\mu_{EC}|^2$ as a function of J for (a) H_2, (b) HD, and (c) D_2.

and two-photon transition moments correlate with each other and with the minima in the energy gaps between the v_E and v_F levels. This correlation supports the conjecture that these variations are the result of resonant tunneling. Only in the comparison of $|M_{fo}|^2$ with $|\mu_{EC}|^2$ for D_2 is there a slight mismatch. Although $|\mu_{EC}|^2$ at $J = 25$ shows a small peak, the corresponding peak for $|M_{fo}|^2$ is at $J = 26$. The source of this discrepancy is the same as for that of the shift of the minimum from $J = 17$ in $|\mu_{EC}|^2$ to $J = 16$ in $|M_{fo}|^2$ for H_2: the concerted nature of the two-photon transition. ΔE for D_2 decreases from $J = 25$ to $J = 26$ [Fig. 9(c)] and, correspondingly, all the contributions to $|M_{fo}|$ increase. However, constructive interfering terms outweigh the destructive ones, which causes $|M_{fo}|$ to increase. The increase of $|M_{fo}|^2$ for D_2 from $J = 25$ to 26 is even more prominent in the $v_X = 1$ and $v_X = 2$ curves (Fig. 5).

The two-level resonant tunneling model in Sec. II predicts that $|\mu_{EC}| = |\mu_{FC}|$ in the limit where $|E_1 - E_2| \ll |V_{12}|$ and the nonresonant transition moments satisfy the inequality $|\mu_{EC}|_{NR} \gg |\mu_{FC}|_{NR}$. Also, the two transition moments at "exact" resonance will be $(2)^{-1/2}|\mu_{EC}|_{NR}$. The $J = 17$ result for HD closely approaches this case. Figure 8(b) shows the near equality of $|\mu_{EC}|$ and $|\mu_{FC}|$. Also, if the value of $|\mu_{EC}|$ at $J = 16$ is used as the nonresonant value, then

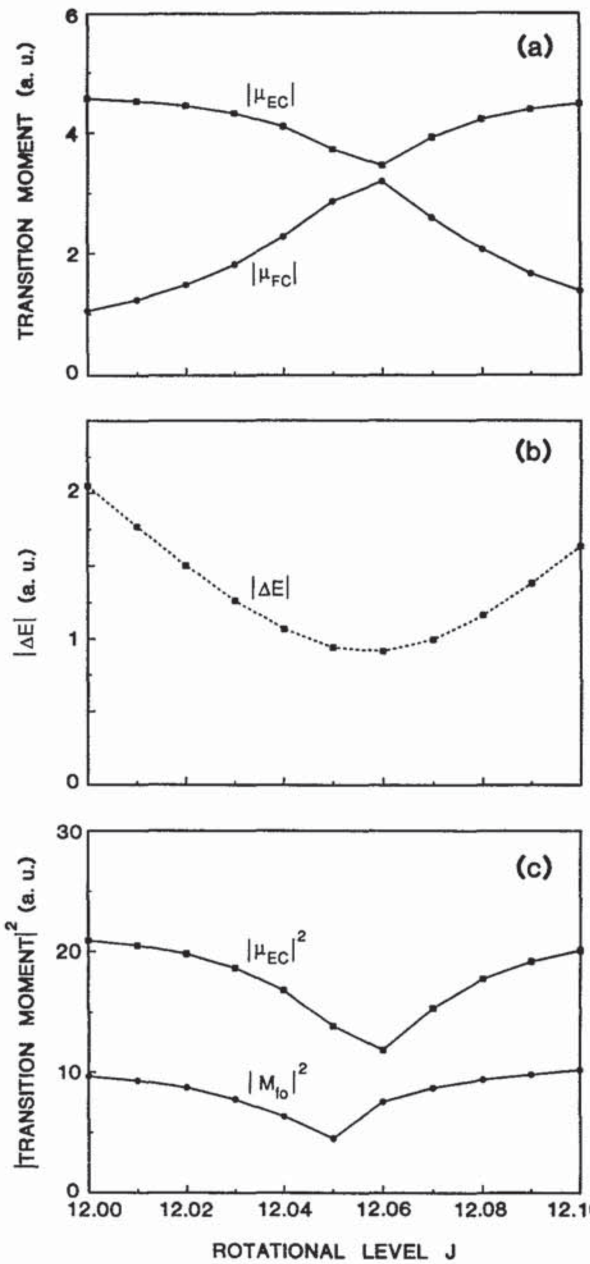

FIG. 11. Shown as a function of J near the $J = 12$ resonance are (a) the magnitudes of the H_2 E–C (0,0) and H_2 F–C (v_F,0) one-photon transition moments, $|\mu_{EC}|$ and $|\mu_{FC}|$, (b) the H_2 energy gap ΔE, and (c) the squares of the H_2 E–X (0,0) two-photon Q-branch transition moment $|M_{fo}|^2$ and H_2 E–C (0,0) one-photon transition moment $|\mu_{EC}|^2$. The v_F level is the one closest to the $v_E = 0$ level for a given J.

$(2)^{-1/2}|\mu_{EC}| = 3.32$ a.u., which should be compared with the calculated value of 3.41 a.u. for $|\mu_{EC}|$ at $J = 17$. This result confirms once more the validity of the resonant tunneling model.

While most of the variations in $|M_{fo}|^2$, $|\mu_{EC}|$, and $|\mu_{FC}|$ are caused by near-resonant tunneling, tuning to exact resonance is possible by modifying the centrifugal potential using fractional values of J, an idea introduced by Senn and Dressler.[12] We use fractional J values to study the behavior of the three transition moments as they approach and then move away from a resonance. In our calculations, a quantal treatment was retained except that J in the centrifugal potential was considered an adjustable parameter, used for tuning the resonance. However, an integer J was used in the calculation of the rotational line strength factor in $|M_{fo}|^2$. This use is acceptable because the rotational line strength factor has no effect on resonant tunneling. We studied the three transition moments at $J = 12.0$ to 12.1 in steps of 0.01 for H_2. This value of J is chosen because the present calculation shows a weak resonance structure at $J = 12$, where the experimental 2 + 1 REMPI result (see Paper II) shows a much more prominent dip.

Figure 11(a) shows the J dependence of $|\mu_{EC}|$ and $|\mu_{FC}|$ near $J = 12$. The two transition moments almost coalesce at $J = 12.06$. Figure 11(b) shows that ΔE is also at a minimum at this J value. Notice that the scale factor multiplying ΔE is 0.25 vs 0.0015 for Figs. 9(a)–9(c). A comparison of $|M_{fo}|^2$ and $|\mu_{EC}|^2$ in Fig. 11(c) shows that, although both transition moments have minima, the two minima are located at slightly different J values. Again this difference can be ascribed to the concerted nature of two-photon transitions. Both $|M_{fo}|^2$ and $|\mu_{EC}|^2$ at their minima are half of their values at $J = 12$, in accordance with the two-level resonance model. The decrease of $|M_{fo}|^2$ by a factor of 2 between $J = 12.0$ to 12.05 clearly indicates the importance of using accurate vibrational potentials in treating resonance tunneling. Indeed, calculations using Born–Oppenheimer potentials gave $|M_{fo}|^2$ at $J = 12$ to be 18% less than the result using adiabatic potentials. Similarly, the present result will also be subjected to changes when nonadiabatic corrections are included. Because the nonadiabatic corrections to the vibrational term values for the E,F state are consistently smaller than the adiabatic corrections,[12,18,21,22] we also expect the nonadiabatic corrections to the resonant tunneling to be smaller than the corresponding adiabatic corrections. The recent study of Quadrelli, Dressler, and Wolniewicz[22] also shows that the vibrational levels of the E,F state acquire a predissociation width caused by the nonadiabatic coupling with the dissociative continuum of the X state. This predissociation width varies strongly with v, but its J dependence is not reported. Although the predissociation does not affect the E–X two-photon absorption directly, it may influence the 2 + 1 REMPI process with the E–X transition as an intermediate step. (See Paper II.)

Figures 3–5 show that, in addition to the sharp dips discussed in the preceding paragraphs, $|M_{fo}|^2$ decreases at high J; the only exception is the $v_X = 2$ result in H_2. At the highest J used in the calculation, the $v_E = 0$ level of H_2 is 143.3 cm^{-1} above the barrier. For HD it is 0.87 cm^{-1} below the barrier, and for D_2 it is 3.4 cm^{-1} above the barrier. Thus all three vibrational wave functions are delocalized and have significant amplitude in the F-well region. This type of delocalization is a result of nonresonant tunneling because it is independent of the relative position of the v_E and v_F levels; it depends only on the distance from the v_E level to the top of the barrier.

IV. CONCLUSIONS

The present study of the v_X, J dependence of the $E\,^1\Sigma_g^+$ $v_E = 0$, J–$X\,^1\Sigma_g^+$, v_X, J transitions demonstrates the concerted nature of two-photon transitions. The J variation furnishes a good probe of resonant tunneling in the double-well potential of the E,F state. We expect this type of J dependence to be consistent for all transitions involving double-well potentials.

ACKNOWLEDGMENTS

K.-D. R. and R. N. Z. thank the National Science Foundation for support under NSF Grant No. CHE 90-07939.

[1] E. E. Marinero, C. T. Rettner, and R. N. Zare, J. Chem. Phys. **80**, 4141 (1984).
[2] R. S. Blake, K.-D. Rinnen, D. A. V. Kliner, and R. N. Zare, Chem. Phys. Lett. **153**, 365 (1988).
[3] K.-D. Rinnen, D. A. V. Kliner, R. S. Blake, and R. N. Zare, Chem. Phys. Lett. **153**, 371 (1988).
[4] K.-D. Rinnen, D. A. V. Kliner, and R. N. Zare, J. Chem. Phys. **91**, 7514 (1989).
[5] D. A. V. Kliner, K.-D. Rinnen, and R. N. Zare, J. Chem. Phys. **90**, 4625 (1989).
[6] D. A. V. Kliner and R. N. Zare, J. Chem. Phys. **92**, 2107 (1990).
[7] D. Robie and W. K. Bischel, Appl. Phys. Lett. **56**, 722 (1990).
[8] K.-D. Rinnen, M. A. Buntine, D. A. V. Kliner, R. N. Zare, and W. M. Huo, J. Chem. Phys. **95**, 214 (1991). This paper is referred to as Paper II.
[9] K.-D. Rinnen, D. A. V. Kliner, R. N. Zare, and W. M. Huo, Israel J. Chem. **29**, 369 (1989).
[10] E. R. Davidson, J. Chem. Phys. **35**, 1189 (1961).
[11] W. Kolos and L. Wolniewicz, J. Chem. Phys. **50**, 3228 (1969).
[12] P. Senn and K. Dressler, J. Chem. Phys. **87**, 1205 (1987).
[13] E. E. Marinero, R. Vasudev, and R. N. Zare, J. Chem. Phys. **78**, 692 (1983).
[14] W. M. Huo and R. L. Jaffe, Chem. Phys. Lett. **101**, 463 (1983).
[15] M. Goeppert-Mayer, Ann. Phys. (Leipzig) **9**, 273 (1931).
[16] R. G. Bray and R. M. Hochstrasser, Mol. Phys. **31**, 1199 (1976).
[17] C. Schwartz and R. J. Le Roy, J. Mol. Spectroc. **121**, 420 (1987).
[18] L. Wolniewicz and K. Dressler, J. Chem. Phys. **82**, 3292 (1985).
[19] L. Wolniewicz and K. Dressler, J. Chem. Phys. **88**, 3861 (1988).
[20] W. M. Huo (unpublished result).
[21] L. Wolniewicz and K. Dressler, J. Mol. Spectrosc. **67**, 416 (1977).
[22] P. Quadrelli, K. Dressler, and L. Wolniewicz, J. Chem. Phys. **93**, 4958 (1990).